A non-enveloped arbovirus released in secretory lysosomes induces super-infection exclusion

Thomas Labadie, Polly Roy[#]

Affiliation: Department of Pathogen Molecular Biology, Faculty of Infectious and Tropical Diseases, London School of Hygiene and Tropical Medicine, Keppel Street, WC1E 7HT, UK

 # Corresponding author: Polly Roy (polly.roy@lshtm.ac.uk)

Short title: Virus released in secretory lysosomes

Abstract

Recent developments on extracellular-vesicles (EVs) containing multiple virus particles challenge the rigid definition of non-enveloped viruses. However, how non-enveloped viruses hijack cell machinery to promote non-lytic release in EVs, and their functional roles, remain to be clarified. Here we used Bluetongue virus (BTV) as a model of a non-enveloped arthropod-borne virus and observed that the majority of viruses are released in EVs, both in vitro and in the blood of infected animals. Based on the cellular proteins detected in these EVs, and use of inhibitors targeting the cellular degradation process, we demonstrated that these extracellular vesicles are derived from secretory lysosomes, in which the acidic pH is neutralized upon the infection. Moreover, we report that secreted EVs are more efficient than free-viruses for initiating infections, but that they trigger super-infection exclusion that only free-viruses can overcome. These results suggest that secreted EVs and free-viruses do not share a common receptor.

Author summary

Recent discoveries of non-enveloped virus secreted in EVs opened the door to new developments in our understanding of the transmission and pathogenicity of these viruses. In particular, how these viruses hijack the host cellular secretion machinery, and the role of these EVs compared with free-virus particles remained to be explored. Here, we tackled these two aspects, by studying BTV, an emerging arthropod-borne virus causing epidemics worldwide. We showed that this virus is mainly released in EVs, *in vivo* and in the blood of infected animals, and that inhibition of the cell degradation machinery decreases the release of infectious EVs, but not free-virus particles. We found that BTV is responsible for neutralizing the pH of lysosomes, which are important organelles of the cell degradation machinery. Our results highlight unique features for a virus released in EVs, explaining how BTV transits in lysosomes without being degraded. Interestingly, we observed that EVs are more infectious than free-virus particles, but only free-viruses are able to overcome the super-infection exclusion, which is a common cellular defense mechanism. In conclusion, our study stresses the dual role played by both forms, free and vesicular, in the virus life cycle.

Introduction

Lipid envelopes surrounding viruses are likely the results of a convergent evolution, potentially acquired during the adaptation of non-enveloped virus to animals [1]. The envelope plays essential roles, such as the fusion with cellular membranes to enter in cells, or the assembly of new virus particles during budding at the plasma membrane. In contrast, non-enveloped viruses developed alternative mechanisms, such as cell entry by membrane penetration [2] and exit by cell lysis. In both cases, free virus particles remain the canonical unit of virus infection, with a single virus particle entering a cell to replicate and amplify its genome. Recent studies in the field of non-enveloped viruses have drawn attention on previously unknown cell-to-cell spread mechanisms, in which released virus particles are not naked. A seminal work on Hepatitis A virus revealed that virus particles are released both in enveloped and non-enveloped states, with the envelope protecting virus particles from neutralising antibodies [3]. More recently, it was reported that other non-enveloped lytic viruses, such as Coxsackievirus B [4], Hepatitis E virus [5], Poliovirus [6,7], Polyomavirus [8,9], Rotavirus and Norovirus [10], can also exit the cells as cloaked in extracellular vesicles (EV). Further, it was observed that EVs could contain multiple virus particles, allowing infection of a unique cell with many virus particles at a time [7,10]. This new transmission mechanism, reported as en block transmission, allows viral genome complementation during the infection and could be a regulator of fitness evolution for a virus population [11,12].

However, the mechanisms by which viruses hijack the host cellular secretion machinery, or the benefit of vesicular transmission are still unclear [11]. Understandings these might alter the rigid definition of non-enveloped viruses. To this end, here we investigated EV associated virus release using a model non-enveloped multi-layered capsid virus, Bluetongue virus (BTV), of the Orbivirus genus, with a segmented double stranded RNA genome. BTV is an insect-borne virus that periodically causes epidemics among ruminants worldwide, with a particularly high mortality rate in sheep. Although classified as a non-enveloped virus, BTV is able to exit cells by both lytic and non-lytic mechanisms [13–15].

Here, we report that EVs containing multiple virus particles are the main infectious unit of BTV. Our results revealed a mechanism of en block transmission in which both MVBs and the late stages of autophagy are essential to cloak virus particles in secreted lysosomes. We demonstrate that EVs are not limited to cell cultures and are found in the blood of animals, and explain how both forms of the virus (free and vesicular) contribute to its life cycle are thus necessary. Indeed, we observed that EV associated virus induces a more efficient infection and synthesis of viral protein than does infection with free virus particles, while free virus particles are essential to overcome super-infection exclusion.

Results

Extracellular vesicles containing multiple virus particles are the main infectious unit

BTV egresses infected cells not only by cell lysis but also by a non-lytic mechanism [13,15]. Since BTV particles were shown to be associated with MVBs components during trafficking [16] and the purified virus particles are associated with NS3 [15], a membrane protein, it is possible that multiple BTV particles are released within EVs. To determine this, we infected sheep cells (PT cell line) and Culicoides insect cells (KC cell line) at a multiplicity of infection (MOI) of 10, and cell culture supernatants were centrifuged to isolate free virus particles from EVs (~1 μm) which sediment as pellets under the conditions used. Virus titrations (Fig 1A) and viral genome quantification by quantitative PCR (Fig 1B) both revealed that the majority of infectious virus particles and viral genomes were sedimented after a 10,000 x g centrifugation. Further, western blot analysis of the structural protein content, both in the pellet and the supernatant revealed that VP2, VP5 and VP7 were at higher levels in the pellet (Fig 1C), consistent with the virus titres. Interestingly, treatment of the total released virus particles (without EVs isolation) from mammalian cells with RNase III was most efficient when combined with both proteinase K and Triton (1%) (Fig 1D), suggesting that a protective membrane is surrounding the virus particles. To localise the BTV proteins within purified EVs, we used a super resolution microscopy approach that could visualise both structural protein VP7 and non-structural protein NS3 with the phosphocholine BODIPY, indicating that BTV is associated

with lipid membranes in EVs (Fig 1E). Moreover, direct observations of both purified EVs secreted from infected cells (Fig 1F), and ultrathin sections of EVs (Fig 1G) by negative stain electron microscopy revealed the presence of large EVs (ranging from 0.5 to 1.5 µm) containing multiple virus particles, corroborating our fluorescence imaging observations. Altogether, these data established that the majority of BTV virus particles are released in large EVs secreted from mammalian and insect infected cells in vitro.

Fig 1. The majority of BTV virus particles are released in large EVs. (A and B) Virus particles (A) and viral genome (B) quantified in the pellet or in the supernatant after isolation of EVs secreted by infected mammalian sheep cells and insect cells. Data are presented as mean ± SD. Each point indicates the value of independent replicates (N = 3; unpaired t-test, *p<0.05, **p<0.01, ***p<0.001, ****p<0.0001). (C) Outer capsid proteins VP2 and VP5, and inner capsid protein VP7, detected in the pellet and supernatant after isolation of EVs secreted by infected mammalian cells. (D) Membrane protection assays on virus particles (EVs and free virus particles) released from infected mammalian cells. Boxplots depict mean and 25–75 percentiles, while whiskers extend from the highest to lowest value (N = 6; unpaired t-test, ***p<0.001, ****p<0.0001). (E) Immunofluorescence microscopy images of purified EVs secreted from infected (two top rows) or mock (bottom row) mammalian cells labelled with anti VP7 (orange) and NS3 (red) antibodies, and a fluorescent lipid membrane marker (green). Scale bar: 2 µm. (F and G) Electron microscopy images of whole EVs (F) and sectioned EVs (G) secreted from infected mammalian cells. Yellow arrows indicate the virus particles positions in the sections. Scale bar: 100 nm.

We also confirmed this phenomenon *in vivo* in bovine blood samples positive for BTV-8 and collected during BTV outbreaks in France in 2019 (Fig 2A). Viral titrations on the EVs and free virus particles fractions separated by differential centrifugation revealed that virus particles were mainly contained within EVs (Fig 2B). However, no significant difference in infectivity between free virus particles and EVs was found in sheep blood samples infected with BTV-1 collected during the 2013 outbreaks. Analysis of purified bovine EVs by transmission electron microscopy showed EVs containing one or more virus particles (Fig 2C) supporting the observation that BTV virus particles are also released within EVs *in vivo*.

Fig 2. EVs containing virus particles are found in the blood of infected bovines. (A and B) Infectivity of EVs and free virus particles released from BTV-1 infected sheep blood (N = 4) (A) and from BTV-8 infected bovine blood (B). Data are presented as mean ± SD. Each point indicates the value of independent replicates (N = 3; unpaired t-test, ns $p>0.05$, *$p<0.05$;). (C) Electron microscopy images of EVs purified from infected bovine blood. Yellow arrows indicate virus particles. Scale bar: 50 nm.

EVs containing multiple virus particles are derived from secretory lysosomes

To determine the origin of EVs containing BTV virus particles, we tested the presence of specific cellular markers. Among the different markers of EVs assessed, we determined the presence of Annexin A2, the tumour susceptibility gene 101 (TSG101), LC3B and the lysosomal associated protein LAMP1 by western blot (Fig 3B). Note that TSG101 is a MVBs marker and LC3B an autophagy-related protein. To identify the cellular mechanisms involved in virus packaging in EVs, we first investigated the potential role of autophagy, using the 3-methyladenin (3-MA) that inhibits class III PI3K activity. We observed that 3-MA failed to significantly decrease the secretion of infectious EVs from sheep cells infected at a MOI of 10 (Fig 3B), suggesting that the induction of autophagy is not essential for the secretion of infectious EVs. However, inhibition of the autophagosome-lysosome fusion with chloroquine (CQ), led to a significant reduction of infectious EVs released as compared to the control (Fig 3B), indicating that the late steps of autophagy are necessary for infectious EVs. In addition, inhibition of MVBs regulator protein HSP90 using geldanamycin in BTV-infected cells (MOI=10) also led to a significant reduction of infectivity measured in the EVs fraction, as compared to the control, indicating a possible role for MVBs in the release of infectious EVs. In contrast, geldanamycin did not affect the levels of free virus particles released. These cumulative inhibitory strategies of autophagy and MVBs provide the evidence that MVBs and late stages of autophagy are both involved in the release of EVs containing virus particles. Following recent description that autophagy and MVBs share common molecular machinery and organelles such as amphisomes [17], we wondered whether EVs could be derived from secreted lysosomes after the fusion with amphisomes. Therefore, the levels of LAMP1 expression within the

cytosol and at the cell surface were measured by flow cytometry (Fig 3C). High levels of cytosolic and surface LAMP1 were detected in infected cells compared with non-infected cells. Interestingly, the ratio of cell surface LAMP1 to cytosolic LAMP1 was also significantly higher in infected cells (Fig 3D), indicating an increase of LAMP1 located at the plasma membrane in infected cells. Moreover, we also examined lysosomes in infected and non-infected cells expressing a LAMP1-GFP fusion protein and in presence of a fluorescent lysotracker specific to acidic organelles (Fig 3E). Confocal microscopy imaging revealed an important decrease of the lysotracker fluorescence intensity in lysosomes of infected cells as compared to control cells, suggesting neutralisation of acidic pH of lysosomes (Fig 3F). However, the number of lysosomes detected in infected cells was significantly higher than in non-infected cells (Fig 3G). Increase of LAMP1 localisation at the plasma membrane and lysosome neutralisation are both hallmarks of an increased lysosomal exocytosis [18,19], indicating that BTV infection reprogram lysosomal degradation pathways to the benefit of lysosomes secretion.

Fig 3. Infectious EVs rely on MVBs and late autophagy. (A) Western blot detection of cellular proteins Annexin A2, TSG101, LC3B and LAMP1 in infected sheep cell lysates and EVs secreted from these cells. (B) Infectivity of the EVs and free virus particles fractions, released from infected sheep cells in presence or absence of 3-MA, geldanamycin or CQ. Data are presented as mean ± SD. Each point indicates the value of independent replicates (N = 3, unpaired t-test, ns $p>0.05$, *$p<0.05$, **$p<0.01$, ***$p<0.001$). (C) Analysis of LAMP1 expression in the cytosol or at the cell surface of sheep cells (mock or BTV infected) by flow cytometry. (D) LAMP1 surface expression ratio, in mock and BTV infected cells. Data are presented as mean ± SD. Each point indicates the value of independent replicates (N = 3, unpaired t-test, **$p<0.01$;). (E) Fluorescence microscopy images of mock and BTV infected sheep cells (MOI = 10) expressing fluorescent fusion protein LAMP1-GFP (green), in presence of an acidic compartment fluorescent marker (red). Scale bar: 10 μm. (F) Fluorescence intensity of the acidic compartment fluorescent marker detected for each lysosome, in BTV or mock infected sheep cells. Violin plots depict min to max values of fluorescence intensity, while the horizontal lines indicate medians (solid lines) and quartiles (dashed lines) (N = 4, with a mean number of lysosomes per replicate of 651.5 ± 149 in mock and 711.5 ± 532 in infected cells; unpaired t-test, ****$p<0.0001$). (G) Average numbers of lysosome/cell in BTV infected and mock sheep cells. Data are presented as mean ± SD. Each point indicates the values of each analysed cell (N = 4, unpaired t-test, **$p<0.01$;).

To provide confirmation, the presence of viral proteins was investigated in the lysosomes of BTV infected cells. Using super resolution microscopy, we observed that outer capsid protein VP5 as well as LAMP1 co-localised with the MVBs marker HSP90, in infected cells only, indicating a fusion between MVBs and the autophagy compartments (Fig 4A). Further, outer capsid protein VP5 as well as NS3 were also co-localised with LAMP1, indicating their localisation within lysosomes (Figs 4B and 4C). To confirm our observations, we used a specific siRNA to knock down the expression of synaptotagmin 7 (syn-7) protein, a key mediator of lysosomal exocytosis. Syn-7 expression was knock down in BSR cells (about 65% decrease, Fig 4D), a widely used cell line for the study of BTV. The amount of infectious EVs released from anti-syn-7 siRNA treated cells were significantly lower, when compared to the untreated BTV-infected BSR cells, from which viruses released predominantly within EVs (Fig 4E; S1A Fig). Therefore, a decrease of syn-7 expression significantly affected virus release within EVs. Further, we observed that inhibition of syn-7 expression did not modify the intracellular replication of BTV at 24 hpi (S1B Fig), showing that the inhibition of syn-7 affected only the release of virus particles. Altogether, our data strongly support that newly synthesised BTV particles are released *via* EVs derived from secretory lysosomes after pH neutralisation.

Fig 4. Infectious EVs are derived from lysosomal compartments. (A-C) Microscopy images of mock or BTV infected sheep cells labelled with anti LAMP1, VP5, HSP90 or NS3 antibodies. Scale bar: 5 µm. Right panels show percentage of VP5 and LAMP1 co-localising with HSP90, and percentage of VP5 and NS3 co-localising with LAMP1 in mock or infected cells. Yellow squares indicate regions with secreted lysosomes shown at higher magnification in (C), scale bar: 2 µm. (D) Western blot detection of GAPDH and syn-7 in BSR cells lysates, in presence or absence of an anti syn-7 siRNA. The ratio of syn-7/GAPDH expression is shown below. (E) Infectivity of EVs and free virus particles fractions, released from infected BSR cells in presence or absence of anti syn-7 siRNA. Data are presented as mean ± SD. Each point indicates the value of independent replicates (N = 3 or 4; unpaired t-test, ns $p>0.05$, *$p<0.05$, **$p<0.01$).

EVs facilitate rapid infection, but only free-viruses can overcome super-infection exclusion

Along with their cellular origin, the role of the secreted form of non-enveloped viruses remain unclear. To better understand the role of EVs during BTV infection, we compared the infectivity of EVs and free virus particles, by analysing the kinetic of total virus production in cells infected either by EVs or free-virus particles. Infection of mammalian cells with infectious EVs or free virus particles led to a similar amount of virus released from cells at 33 hours post infection (hpi). However, at 9 hpi, we found that cells infected with infectious EVs released more virus (Fig 5A), and presented a higher level of viral genome in their cytoplasm (Fig 5B) than cells infected with free virus particles. This suggests that infectious EVs are a more efficient form of infecting agents than are free virus particles. To test this possibility, we investigated the kinetic of viral protein synthesis by following the formation of viral inclusion bodies (VIBs, virus assembly factories) in the cytosol of cells infected with either EVs or free virus particles (MOI = 10). We examined the size and number of VIBs in infected cells between 6 to 21 hpi, by fluorescence microscopy (Fig 5C). A frequency analysis of the VIBs surfaces distribution (Fig 5D and 5E) revealed that at 6 hpi, VIBs median surfaces were 31.36 μm^2 (range: 22 to 63.84 μm^2) in free-virus infected cells against 35.04 μm^2 (range: 22.16 to 78.12 μm^2) in EVs infected cells. At 12 hpi, VIBs mean size surface was clearly smaller in free-virus infected cells with 31.60 μm^2 (range: 22 to 70.72 μm^2) as compared to EVs infected cells (44.52 μm^2, range: 22 to 123.44 μm^2). This result suggests that virus-directed protein synthesis is considerably more efficient in EV infected cells, plausibly due to the higher number of viral genomes entering the cells. An analysis of the frequency distribution of VIBs formed per cell at 6 hpi (Fig 5F) indicated that EVs infected cells had a geometric mean of 2.7 VIBs/cell whereas in free-virus infected cells, the geometric mean was 1.1 VIBs/cell, supporting the idea that infectious EVs allow the formation of multiple viral factories soon after the infection. Together, these data indicate that EV infected cells produce more VIBs, that expand faster, than VIBs produced by free-virus infected cells. Thus, in addition to containing the majority of infectious virus particles released from infected cells, EVs are also more efficient than free-virus particles to initiate an infection.

Fig 5. Infection with EVs is more efficient than infection with free virus particles. (A) Kinetics of free virus particles and EVs release from infected sheep cells. (B) Kinetics of viral RNA replication in sheep cells infected with total virus particles, EVs or free virus particles. Each point indicates the means relative titre (percentage of maximum reached infectivity) and vertical lines represent the SDs (N = 3; unpaired t-test between EVs and free virus particles values, *$p<0.05$). (C) Microscopy images of sheep cells infected with infectious EVs (left panel) or free virus particles (right panel) at 6 hpi (upper panel) or 21 hpi (lower panel). For each condition a merge of the plasma membrane fluorescent marker (WGA, green) with nucleus staining (blue) and viral NS2 labelling (red), or the NS2 labelling only is shown. Scale bar: 10 µm. (D) Frequency distribution of VIB surfaces (μm^2) measured in EVs or free virus particles infected cells between 6 and 21 hpi. (E) Kinetics of VIBs surface growth in sheep cells infected with either EVs or free virus particles, derived from the frequency distribution shown in (C). Points indicate the geometric mean surface and vertical lines represent the geometric standard deviation factor. (F) Frequency distribution of the VIBs number/cells, after 6 hours of infection with EVs or free virus particles. Points represent the number of cells, lines represent the log normal regression analysis of the cell distributions ($R^2 = 0.98$) and the shaded area represent the confidence interval (95%).

We next considered if differences between EVs and free virus particles are due to cell defence mechanisms, such as super-infection exclusion. Although not always understood, this cell defence mechanism in which infected cells become resistant to a second infection has been observed for several viruses. We first evaluated the presence of a super-infection exclusion mechanism in sheep cells infected with BTV, using two different viruses, a non-modified BTV (BTV_{WT}) and a fluorescent BTV (BTV_{UnaG}) encoding a fluorescent fusion protein VP6-UnaG. After controlling that BTV_{UnaG} virus particles are also mainly released in EVs (Fig 6A), we first infected sheep cells with $BTV_{WT,}$ followed by a second infection with BTV_{UnaG} immediately (0 hpi) or at 1, 2, 3, 4 or 5 hpi (Fig 6B). 12 hours after the initial infection, cells were then labelled with an anti VP6 antibody (to detect VP6 produced by both viruses), whereas UnaG detection allowed the detection of the BTV_{UnaG} virus only (Fig 6C). Flow cytometry analysis coupled with a gating strategy allowed us to differentiate non-infected versus infected cells with one or two different viruses (Fig 6D). A strong decrease of the UnaG fluorescence was observed in cells with the longer incubation times between the two

infections (Fig 6E). This result provides evidence that BTV infection induces super-infection exclusion in sheep cells. We repeated this experiment by infecting sheep cells with BTV_{WT} (total virus particles), and then with free-virus particles or EVs of BTV_{UnaG}. Sheep cells were first infected with BTV_{WT}, and then BTV_{UnaG} free virus particles or infectious EVs. A super infection exclusion mechanism was observed in cells co-infected with BTV_{WT} and EVs containing BTV_{UnaG} (Fig 6F), with an important decrease of UnaG fluorescence intensity dependent on the incubation times between the two infection. Conversely, no significant differences of UnaG fluorescence were detected in cells with secondary infection of BTV_{UnaG} free virus particles over time (Fig 6G). Altogether, these results indicate that while BTV infection led to a super-infection exclusion mechanism in sheep cells, BTV free virus particles were able to overcome this mechanism.

Fig 6. Only free virus particles overcome super-infection exclusion. (A) Infectivity of EVs and free virus particles fractions, released from sheep cells infected by BTV_{UnaG}. Data are presented as mean ± SD. Each point indicates the value of independent replicates (N = 3; unpaired t-test, **p<0.01). (B) Experimental design. Sheep cells were first infected with BTV_{WT}, followed by BTV_{UnaG} infection at 0, 1, 2, 3, 4 or 5 hpi. VP6 quantification was performed at 12 hpi. (C) Microscopy images of mock or BTV_{UnaG} infected cells labelled with a VP6 antibody (red). VP6-UnaG (green) and nucleus (blue) were also detected. Scale bar: 10 µm. (D) Gating strategy for discrimination of sheep cells infected with BTV_{WT} only, BTV_{UnaG} only, both BTV_{WT} and BTV_{UnaG}, or non-infected cells, during flow cytometry analysis. Non-infected cells are present in the lower left gate, BTV_{WT} infected cells in the upper left gate, BTV_{UnaG} infected cells in the lower right gate, and cells infected with both virus in the upper right gate. (E-G) Relative UnaG fluorescence (percentage of UnaG fluorescence at 7 hpi) after primary infection with BTV_{WT} and a secondary infection with either total BTV_{UnaG} (free virus particles and EVs) (E), EVs of BTV_{UnaG} (F) or free virus particles of BTV_{UnaG} (G). Data are presented as geomean ± geometric standard deviation factor. (N = 3; ANOVA, ns p>0.05, *p<0.05, **p<0.01, ***p<0.001, ****p<0.0001).

Discussion

While recent discoveries regarding EVs containing viruses have changed our perception of non-enveloped viruses, such observations were lacking for a non-enveloped arthropod-borne virus. Moreover, it has been hypothesised that lipid envelopes are the hallmark of virus adaptation to animals [1]. Among all the arthropod-borne viruses infecting vertebrates, arthropod-borne reoviruses are the only non-enveloped viruses. Based on these results and the recent literature on picornavirus, polyomavirus, calicivirus and rotavirus [3,7,10,20], it is tempting to suggest that the vesicular transmission could be another example of convergent evolution for a non-enveloped virus adapting to animals. In this study, we demonstrated that the majority of BTV virus particles are clustered in EVs, secreted by both mammalian and insect cells. This phenotype was observed for at least two different serotypes, BTV-1 in cell culture and BTV-8, in the blood of contaminated bovines. Despite the absence of envelope, our results highlight the presence of a lipid bilayer protecting virus particles and providing a more efficient entry mechanism compared with free virus particles infection.

It has been reported that Hepatitis A virus and hepatitis E virus exit cells inside exosomes derived from the MVBs [3,5,21], that are characterised by the presence of endosomal compartments and vesicular transport markers, such as Flotillin 2, CD63 or members of the ESCRT protein family. These exosomes are around 50-200 nm in size [22]. In contrast, it has been shown that Coxsackievirus B and Poliovirus are released in EVs ranging from 50 nm to 2 µm, through an autophagy-mediated mechanism [4,6,7]. Moreover, a recent study reported that Rotavirus and Norovirus egress cells in EVs derived from the plasma membrane, independently of MVBs and autophagy [10]. A clear picture of different mechanisms used by non-enveloped virus for secretion in EVs is lacking. Our study contributes to understand better the diversity of release mechanisms

We showed that the lysosomal marker LAMP1 is present in infectious EVs, in addition to the MVB marker TSG101. This suggests that after the fusion between MVBs and autophagosome leading to the recently discovered secretory amphisome [17], virus particles could be subsequently exported in

lysosomes after the amphisomes-lysosomes fusion. Our data provide an original description of a virus particles release mechanism through secretory lysosomes. Interestingly, this phenomenon is not restricted to viruses, as it has also been described for intracellular uropathogenic E. coli [19]. Additionally, we also showed that EVs containing virus particles offer an efficient platform for entry and infection of naive cells. However, we observed that BTV infection triggers a superinfection exclusion phenomenon for EVs containing virus particles, whereas free virus particles can overcome it, underlying the importance of both viral forms during BTV cycle.

Previously, we showed BTV VP2, the outer capsid spike binds sialic acid, a likely receptor for the free virus particles [23]. However, reports from others showed that infection with virus particles cloaked in EVs did not necessarily rely on their known virus receptor [7,8,20,24]. Here, we discovered a super-infection exclusion mechanism during BTV infectious, supporting the existence of a specific EV receptor. We observed that only free virus particles could enter in cells already infected, suggesting that EVs and free virus particles use different entry routes. In such a scenario, the receptor is not required to interact with viral outer capsid proteins, as EV secretion is already an efficient cell-to-cell communication system [25]. However, the difference in virus tropism would certainly have consequences on the virus pathogenicity. It is thus necessary to study the impact of infectious EVs on BTV induced pathogenicity, as infected ruminants variably respond to BTV infection, with cattle being mainly asymptomatic and sheep exhibiting more severe clinical signs, such as haemorrhage and ulcer in the gastro-intestinal tract or muscle necrosis [26]. In this study, we were able to identify infectious EVs in the blood of bovines infected in 2019, but it was not possible to obtain any evidence of infectious EVs in blood samples of infected sheep. However, it may be also possible that the long storage of the sheep blood samples used in this study might have affected EVs in sheep blood. In natural hosts, BTV transmission requires blood feeding midges (Culicoides species) to take a blood meal from an infected animal. Our results demonstrated that Culicoides cells, for which BTV is not cytopathic, also secrets EVs containing virus particles. It would be thus

interesting to investigate whether the uptake of EVs secreted by infected insects and EVs secreted by infected mammals can infect in mammals or insects respectively.

Overall, the findings described here highlight an original aspect of virus release leading to the secretion of a non-enveloped virus in host-derived secretory lysosomes, of which the acidic pH is neutralized upon the infection. Such mechanism is distinct to the proposed mechanism for the release of rotavirus in EVs [10], suggesting a divergent evolution of insect-borne double-stranded RNA viruses. Investigation of host-pathogen interactions for insect-borne viruses can significantly enhance our knowledge on the diversity of virus-containing extracellular vesicles origins. This may highlight different cellular tropisms and immunity evasion strategies between the free and vesicular forms of non-enveloped viruses, and can have important implications for the development of innovative approaches for virus control.

Acknowledgements

The authors are very grateful to Stephan Zientara and Corinne Sailleau for providing the animal blood samples (BTV national reference centre, ANSES, Maisons-Alfort, France). We also thank Eiko Matsuo (Kobe University, Kobe City, Japan) for providing the BTV_{UnaG} fluorescent virus. We acknowledge microscopy support from Mark Turmain (The Biosciences EM core facility, UCL, London UK). This research was funded by a Wellcome Trust senior investigator award to Polly Roy (100218/Z/12/Z).

Author contribution

TL generated all the experimental data. TL and PR interpreted the data and wrote the manuscript.

Declaration of interests

The authors declare no competing interests.

Material and Methods

Cell lines and virus stocks

BSR cells (a derivative of the Baby Hamster Kidney cells BHK21 [27]) and PT cells (a sheep kidney cell line [28]) were maintained in Dulbecco's Modified Eagle's Medium (DMEM) (Sigma Aldrich), supplemented with 5% foetal calf serum (FCS) and antibiotics (100 units/mL penicillin, 100 mg/mL streptomycin, GIBCO, Life Technologies). KC cells (A Culicoides insect derived cell line) were maintained in Schneider′s Insect Medium (Sigma Aldrich), supplemented with 10% FCS and antibiotics (100 units/mL penicillin, 100 mg/mL streptomycin, GIBCO, Life Technologies). Mammalian cells were incubated at 35°C in a humidified 5% CO2 incubator and insect cells at 28°C. BTV-1 and BTVUnaG (with a segment 9 encoding a VP6-UnaG fusion protein) stocks were obtained by infecting sheep cells at a multiplicity of 10 plaque forming units per cell (pfu/cell) for 30 min under gentle agitation at room temperature (RT). The inoculum was then removed and cells were maintained for 48 h in DMEM with 2% FCS for 48 h at 35°C. The harvested supernatants were

clarified (10 min at 500xg) twice, and stored at 4°C. All the NS3 mutants were described in previous studies [14,15,29,30]. Stocks for these mutants were amplified as described above for BTVWT, and a sanger sequencing of NS3 confirmed the presence of all studied mutations.

Virus titration and replication kinetic

Viral infectivity was estimated using tissue culture infectious dose of 50 per mL ($TCID_{50}$/mL) titration, for which viral suspensions were diluted from 10−1 to 10−12 in D-MEM medium and inoculated to BSR cells in 96-well plates. Titres were calculated according to the Spearman-Karber method. For analysis of replication, sheep cells were inoculated with purified EVs or free virus particles in 6-well plate (MOI = 1) for 1 h at RT under gentle rotation. The inoculum was then removed and replaced by D-MEM (1% FCS). Cell culture media was harvested at 9, 24, 33 and 48 hpi, clarified by centrifugation (500xg – 10 min), and infectivity was quantified by a $TCID_{50}$ method. PT infected cells were lysed by three cycle of freeze thawing. Lysed cells were resuspended in PBS and cell debris was spun down at 500 g for 5 min. Viral RNA extraction was then performed on the harvested supernatant as indicated below.

Viral genome quantification

Extraction of the viral RNA was performed with a Qiamp viral RNA mini kit (Qiagen), followed by a reverse transcription using a universal degenerated oligo specific to all 5′ non-coding sequences of BTV-1 segments (BTV/Uni1; 5′ GTTAAAWHDB 3′) and the GoScript Reverse Transcription System (Promega, Madison, WI, USA). The cDNAs obtained for the segment 7 were then quantified with a real time quantitative PCR, using the 2x SYBR Green qPCR Master Mix (Bimake, Houston, TX, USA) and segment 7 specific primers (BTV1 S7/322F, 5′ GACGCCAGAGATACCTTTTAC 3′; BTV1 S7/478R, 5′ CTTGAATCATATCCGGACCAC 3′). For absolute quantification of the cDNA copy numbers, a standard curve was produced using a 10-fold serial dilution of a pT7-S7 plasmid of known concentration as a template for amplification.

Isolation of EVs

EVs were isolated from infected cells cultured in DMEM 1% FCS (mammalian cells) or Schneider′s Insect Medium (10% FCS), except for the analysis of protein markers in EVs by western blot and immunofluorescence, for which cells were cultured in 0% FCS medium in order to avoid detection of EVs present in the FCS. Following harvesting of the cell culture supernatant after 24 hours of infection, EVs were purified from free virus particles using a differential centrifugation protocol adapted from one used on encephalomyocarditis virus [31]. Cell debris was first removed by two steps of low speed centrifugation at 500xg for 10 min. Large EVs were pelleted by centrifuging initial volumes of 1.5 ml at 10,000xg for 30 min. Free virus particles remained in the supernatant, and pelleted EVs were resuspended in 50 µL D-MEM without FCS for subsequent analysis. EVs were purified from frozen blood samples by a similar method. First, samples were quickly defrosted at 37°C, then 500 µL volumes of blood were diluted in sterile PBS (1:3) (BR0014G, Thermofisher Scientific) and centrifuged at 500xg for 10 min, followed by a 2000xg centrifugation step for 10 min in order to completely removed lysed erythrocytes. Finally, a 10,000xg centrifugation step was performed for 30 min and the pellet was resuspended in 60 µL PBS. All centrifugation steps were performed at 4°C.

Western Blot

Proteins were detected from either resuspended EVs or cell lysates. Cell monolayers were washed twice with a PBS solution and lysed for 30 min at 4°C with a RIPA lysis buffer, 1X protease inhibitor cocktail, and 5 mM EDTA (78438, Thermofisher scientific). Cell lysates, or EVs, were diluted in 2X Laemli buffer (1:1) and incubated at 95°C for 5 min. Proteins were then separated on a 10% SDS gel and blotted on a PVDF membrane. When indicated, the membranes were cut horizontally for incubation with different antibodies. The anti VP2, VP5 and VP7 antibodies (made in the Pr. Roy's laboratory [32]), anti LC3B (NB600-138455, Novus Bio), anti synaptotagmin 7 (105-173, Synaptic system), anti GAPDH (ab9485, Abcam), anti annexin A2 (610069, BD Bioscience), anti TSG101 (sc-6037, Santa Cruz Biotechnology) and anti LAMP1 (ab24170, Abcam) were incubated overnight at

4°C, followed by a 2 hours incubation with respective Horseradish peroxidase-coupled secondary antibody (anti-mouse IgG ab97023, anti-guinea pig IgG ab97155 and anti-rabbit IgG ab97051, Abcam). Luminescence was then detected using SuperSignal West Pico PLUS Chemiluminescent Substrate (Thermo Fisher Scientific). The ImageJ software was used to perform linear contrast enhancement and protein semi quantification.

Membrane protection assay

Viral supernatants containing free virus particles and EVs were harvested from sheep cells 24 hpi. Virus particles were treated with a solution of PBS-triton-x100 at final concentration of 1% (T9284, Sigma Aldrich) for 30 min at RT, and/or proteinase K at 5 µg/mL final (P4850, Sigma Aldrich) during 1 hour on ice followed by a 1x protease inhibitor cocktail containing AEBSF (78438, Thermofisher scientific) treatment for 5 min on ice to deactivate the proteinase K. Finally, virus particles were treated with the double stranded RNA specific RNAse III (1 U/µL final) (AM2290, Thermofisher scientific) for 3 hours at RT. The remaining viral genome was then quantified as described above.

Transmission electron microscopy

To image EVs without sectioning, purified EVs were resuspended in D-MEM, adsorbed onto a carbon-coated copper grid, and stained with a 1% solution of uranyl acetate. For imaging of EVs sections, purified EVs were resuspended in 30 µL D-MEM (0% FCS) and mixed with a low volume of Glutaraldehyde 25% (final concentration = 2.5%) (16220, Electron Microscopy Sciences). After 10 min of fixation at RT, EVs were briefly warmed to 37°C, and 16 µL of EVs were dropped on 4 µL of pre-melted low-melting agar (5% in water) and kept at 42°C before the addition of EVs. Samples were quickly mixed by pipetting and stored at 4°C before sectioning. After post-fixation in 1% osmium tetroxide—0.1% sodium cacodylate, EVs were dehydrated in increasing concentrations of ethanol and embedded in epoxy resin (TAAB Laboratories Equipment Ltd., Aldermaston, United Kingdom). Ultrathin sections were stained with Reynolds lead citrate and mounted onto nickel grids. Images were visualised with a transmission electron microscope (JEM-1400, JEOL Akishima, Tokyo, Japan).

Animal blood samples

Bovine and ovine blood samples were generously provided by the French national reference centre (Maisons-Alfort, ANSES). Sheep showing clinical signs in Corsica were sampled in 2013 [33], and bovines showing clinical signs in the south-west of France were sampled in 2019 [34]. A PCR-based diagnostic performed at the time of the blood sampling confirmed the infection of sheep with BTV-1 and bovines with BTV-8. Blood were then kept frozen until reception by us, for subsequent EVs isolation.

siRNA-mediated inhibition of gene expression

PT cells or BSR cells were reverse transfected with 400 nM Silencer Negative Control No. 1 siRNA (AM4611; Ambion) or with a synaptotagmin 7 Silencer predesigned pool of 4 siRNA (L-004306-02-0005; Dharmacon) using the Lipofectamine RNAiMAX transfection reagent (13778-100; Invitrogen). Transfections were carried out according to the supplier's instructions (ratio 3:1). Cells were transfected for 48 h prior to BTV1 infection (MOI = 10).

Drugs-mediated inhibition of EVs release

Sheep cells in 6 well-plates were infected (MOI = 10) with BTV-1, 24 hours post seeding. Viral or mock inoculum were incubated 30 min at RT under gentle rotation. The inoculum was then removed and replaced by D-MEM (1% FCS), and cells were incubated at 35°C in a humidified incubator (5% CO_2). At 1 hpi, cell culture medium was replaced with D-MEM containing 10 mM 3-methyladenine (M9281, Sigma Aldrich), 300 nM geldanamycin (InvivoGen) or 20 µM chloroquine (C6628, Sigma Aldrich), so that drugs did not interfere with viral entry. These concentrations were selected because they were already validated by previous studies on BTV from us and others [35,36]. At 24 hpi, cell supernatant were harvested for isolation of EVs and analysis of infectivity. For intracellular virus particle quantification in presence or absence of geldanamycin, the media culture of PT infected cells was removed at 24 hpi, and cell monolayers were rinsed twice with PBS. Cells were then lysed by 3 successive cycles of freeze/thaw at -80°C/37°C. Cell lysates were then resuspended in DMEM and virus particles quantified using a $TCID_{50}$ method.

Quantification of cell surface proteins

Cell surface protein expression of LAMP1 was measured by immunofluorescence using flow cytometry. PT cells were seeded in 6-well plates for 24 h before infection with BTV-1 (MOI = 10). After 24 hpi, cell monolayers were washed twice with PBS, re-suspended using trypsin-EDTA (Thermo Fisher Scientific) and fixed with paraformaldehyde 2% (w/v) for 10 min. For each replicate, PT cells were then split in two separate tubes. Cells permeabilisation was performed with a solution of PBS-Triton x100 (0.05% v/v) for 5 min in only one of the two tubes, allowing quantification of total protein content in the permeabilised cells and cell surface protein only in non-permeabilised cells. The cells were then blocked using bovine serum albumin (PBS-BSA 1%) for 30 min and incubated with rabbit anti LAMP1 (ab24170, Abcam) and guinea pig VP5 antibodies overnight at 4°C, and incubated for 2 h at RT in the presence of a species-specific Alexa Fluor A633 and A488 conjugated secondary antibodies (A21071 and A11073, Thermo Fisher Scientific). After centrifugation and washing, cells were re-suspended in PBS and analysed with a BD LSR II flow cytometer (BD Biosciences, San Jose, CA, USA). For each replicate, 30,000 cells were analysed using the same parameters. Flow cytometry data were analysed with FlowJo (FlowJo LLC, Ashland, OR, USA) software. For the analysis, a gating strategy discriminating doublet cells by plotting FSC-A vs. FSC-H was used, and VP5 positive cells were selected using mock-infected cells stained the same way to determine the threshold of background fluorescence.

Fluorescence microscopy

For imaging, EVs were resuspended in D-MEM (0 % FCS) + fluorescent Bodipy Phosphocholine analogue at 2 µg/mL (D3793, Thermofisher Scientific) and incubated overnight at 4°C. EVs were then dropped on poly-L-Lysine (P4707, Sigma Aldrich) pre-coated chambered #1.0 Borosilicate coverslips (Nunc Lab-Tek 155411, Thermofisher Scientific), and adsorbed for 1 hour at 37°C. The residual medium was removed, and attached EVs were fixed with PBS-PFA (2%) for 10 min at RT, rinsed with PBS and permeabilised with PBS-triton X100 (0.05%) for 5 min at RT. EVs were then rinsed twice with PBS, incubated for 1 hour at RT with a solution of PBS-BSA (1%), and incubated

overnight at 4°C with primary antibodies anti VP7 and NS3 (made in Pr. Roy's laboratory) and anti CD63 (Ab118307, Abcam), followed by fluorophore A633 and A546-conjugated antibodies (A21071 and A11074, Thermofisher Scientific) for 2 hours at RT and mounting with aqueous mounting medium (F4680, Sigma Aldrich).

For sheep cells imaging, cells were cultured in chambered tissue culture treated polymer coverslips (µ-slide Angiogenesis 81506 or µ-slide 4 well 80427, Ibidi), infected with BTV-1 (MOI = 10) 24 h post-seeding, and at 1 hpi, inoculated with a baculovirus encoding LAMP1-GFP at concentration of 10 particles / cell (CellLight Lysosomes-RFP, BacMam 2.0, Thermofisher scientific). At 18 hpi (unless specified), cell monolayers were rinsed twice in PBS, fixed in PBS-PFA (2%) for 10 min, permeabilised in PBS-triton X100 (0.05%) for 5 min, incubated in PBS-BSA (1%) for 30 min. Cells were labelled with primary antibodies anti HSP90 (11405-1-AP, Proteintech), anti VP5 and anti NS3 overnight at 4°C, and labelled with Alexa fluor A488, A546 and A633-conjugated antibodies (A11001, A11074 and A21071, Thermofisher scientific) for 2 hours at RT. Nuclei were labelled with a PBS-Hoescht solution at 2 µg/mL for 5 min at RT and samples were finally mounted in mounting medium (F4680, Sigma Aldrich). Labelled cells and EVs were analysed with an inverted LSM 880 confocal microscope with airyscan (Carl Zeiss Ltd.), or with an inverted widefield Nikon Ti Eclipse microscope (Nikon) for the VIBs surface analysis. For the co-localisation analysis, three independent replicates (with more than 90 cells imaged for each replicate) were analysed with a Statistical Object Distance Analysis (SODA) on the whole cells [37].

Lysosomal pH investigation

After infection with BTV-1 (MOI = 10), cells were incubated at RT under gentle rotation for 30 min, before the inoculum was replaced with D-MEM containing baculovirus expressing LAMP1-GFP at concentration of 10 particles / cell (CellLight Lysosomes-RFP, BacMam 2.0, Thermofisher scientific). At 18 hpi, cells were incubated with Hoescht at 2 µg/mL for 5 min at RT, followed by an acidic compartment marker 100 nM (Lysotracker DND199, Thermofisher scientific) for 1 min at RT. Cells were then washed twice with a PBS solution and analysed with a LSM880 confocal microscope.

Images were analysed with Icy (https://icy.bioimageanalysis.org). Cells were counted by detection of stained nuclei and lysosomes by detection of the fusion LAMP1-GFP fluorescent protein. Each lysosome detected was considered as a region of interest, and Lysotracker fluorescence intensity detected in these regions were then quantified.

Monitoring of VIBs during the infection

Cells were infected and fixed at different times post infection as above, and labelled with an anti NS2 (made in Pr. Roy laboratory) antibody, a secondary Alexa fluor A546-conjugated antibody (A11074, Thermofisher scientific), and A488-conjugated wheat germ agglutinin as a membrane label (W11261, Thermofisher scientific) for 10 min at RT prior cells permeabilisation. Microscopy images were analysed with Icy, and VIBs were detected using the spot detector plugin, which provided NS2 spot surfaces. Cell counting was performed based on the number of nuclei detected in images. For data analysis, a cut-off was applied to keep all detected NS2 spots with a surface above 22 μm^2. The frequency distribution of VIBs surface values were performed with a bin width of 15 μm^2 and the lognormal regression of the frequency distribution of the number of VIBs per cells were performed after confirming that data were following a lognormal distribution. The total number of VIBs measured at each time points is indicated in the S1 table.

Super-infection exclusion analysis

For superinfection exclusion analysis, sheep cells in 6 well-plates were infected with BTV-1 (BTV_{WT}, MOI = 5) as described above. Simultaneously (0 hpi), or at 1, 2, 3, 4 or 5 hpi, cells were inoculated with purified EVs or free virus particles of BTV_{UnaG} (MOI = 5) and placed at 35°C in a humidified incubator (5% CO_2) for 1 hour. BTV_{UnaG} inoculum was then removed and replaced with D-MEM (1% FCS). At 12 hpi (7 hpi of BTV_{UnaG} infection), cell monolayers were washed twice with PBS, re-suspended using trypsin-EDTA (Thermo Fisher Scientific), fixed with paraformaldehyde 2% (w/v) for 10 min, permeabilised with a solution of PBS-Triton x100 (0.05% v/v) for 5 min, and blocked with a PBS-BSA (1%) solution for 30 min. The cells were then incubated with an anti VP6 antibody (made in Pr. Roy's laboratory) overnight at 4°C, followed by an incubation of 2 h at RT in the

presence of a species-specific Alexa Fluor A633 conjugated secondary antibodies (A21071, Thermo Fisher Scientific). After centrifugation and washings, cells were re-suspended in PBS and analysed with a BD LSR II flow cytometer (BD Biosciences, San Jose, CA, USA). For each replicate, 30,000 cells were analysed using the same parameters. The detection of Alexa Fluor 633 fluorescence corresponded to the total VP6 detected in infected cells, and the UnaG detected fluorescence to VP6 expressed by BTV_{UnaG} infection only.

Statistical analysis

Numerical data were analysed with Prism software version 8.1.2 (Graph Pad Software, San Diego, CA, USA). For all sets of data, equal variances across samples were investigated (Bartlett's test), and according to the number of samples, two-tailed t-tests or ANOVA tests were performed for statistical comparison.

Data availability

The data that support the findings of this study are available from the corresponding author upon reasonable request.

References

1. Buchmann JP, Holmes EC. Cell Walls and the Convergent Evolution of the Viral Envelope. Microbiol Mol Biol Rev. 2015;79: 403–418. doi:10.1128/MMBR.00017-15

2. Spriggs CC, Harwood MC, Tsai B. How non-enveloped viruses hijack host machineries to cause infection. Adv Virus Res. 2019;104: 97–122. doi:10.1016/bs.aivir.2019.05.002

3. Feng Z, Hensley L, McKnight KL, Hu F, Madden V, Ping L, et al. A pathogenic picornavirus acquires an envelope by hijacking cellular membranes. Nature. 2013;496: 367–371. doi:10.1038/nature12029

4. Robinson SM, Tsueng G, Sin J, Mangale V, Rahawi S, McIntyre LL, et al. Coxsackievirus B Exits the Host Cell in Shed Microvesicles Displaying Autophagosomal Markers. PLOS Pathogens. 2014;10: e1004045. doi:10.1371/journal.ppat.1004045

5. Nagashima S, Jirintai S, Takahashi M, Kobayashi T, Tanggis, Nishizawa T, et al. Hepatitis E virus egress depends on the exosomal pathway, with secretory exosomes derived from multivesicular bodies. Journal of General Virology,. 2014;95: 2166–2175. doi:10.1099/vir.0.066910-0

6. Bird SW, Maynard ND, Covert MW, Kirkegaard K. Nonlytic viral spread enhanced by autophagy components. Proc Natl Acad Sci U S A. 2014;111: 13081–13086. doi:10.1073/pnas.1401437111

7. Chen Y-H, Du W, Hagemeijer MC, Takvorian PM, Pau C, Cali A, et al. Phosphatidylserine Vesicles Enable Efficient En Bloc Transmission of Enteroviruses. Cell. 2015;160: 619–630. doi:10.1016/j.cell.2015.01.032

8. Morris-Love J, Gee GV, O'Hara BA, Assetta B, Atkinson AL, Dugan AS, et al. JC Polyomavirus Uses Extracellular Vesicles To Infect Target Cells. mBio. 2019;10: e00379-19. doi:10.1128/mBio.00379-19

9. Handala L, Blanchard E, Raynal P-I, Roingeard P, Morel V, Descamps V, et al. BK Polyomavirus Hijacks Extracellular Vesicles for En Bloc Transmission. Journal of Virology. 2020;94. doi:10.1128/JVI.01834-19

10. Santiana M, Ghosh S, Ho BA, Rajasekaran V, Du W-L, Mutsafi Y, et al. Vesicle-Cloaked Virus Clusters Are Optimal Units for Inter-organismal Viral Transmission. Cell Host & Microbe. 2018;24: 208-220.e8. doi:10.1016/j.chom.2018.07.006

11. Altan-Bonnet N, Perales C, Domingo E. Extracellular vesicles: Vehicles of en bloc viral transmission. Virus Research. 2019;265: 143–149. doi:10.1016/j.virusres.2019.03.023

12. Shirogane Y, Watanabe S, Yanagi Y. Cooperation between different variants: A unique potential for virus evolution. Virus Research. 2019;264: 68–73. doi:10.1016/j.virusres.2019.02.015

13. Hyatt AD, Gould AR, Coupar B, Eaton BT. Localization of the non-structural protein NS3 in bluetongue virus-infected cells. Journal of General Virology. 1991;72: 2263–2267. doi:10.1099/0022-1317-72-9-2263

14. Celma CCP, Roy P. A Viral Nonstructural Protein Regulates Bluetongue Virus Trafficking and Release. J Virol. 2009;83: 6806–6816. doi:10.1128/JVI.00263-09

15. Labadie T, Jegouic S, Roy P. Bluetongue Virus Nonstructural Protein 3 Orchestrates Virus Maturation and Drives Non-Lytic Egress via Two Polybasic Motifs. Viruses. 2019;11: 1107. doi:10.3390/v11121107

16. Bhattacharya B, Celma CC, Roy P. Influence of Cellular Trafficking Pathway on Bluetongue Virus Infection in Ovine Cells. Viruses. 2015;7: 2378–2403. doi:10.3390/v7052378

17. Xu J, Camfield R, Gorski SM. The interplay between exosomes and autophagy – partners in crime. J Cell Sci. 2018;131: jcs215210. doi:10.1242/jcs.215210

18. Machado E, White-Gilbertson S, Vlekkert D van de, Janke L, Moshiach S, Campos Y, et al. Regulated lysosomal exocytosis mediates cancer progression. Science Advances. 2015;1: e1500603. doi:10.1126/sciadv.1500603

19. Miao Y, Li G, Zhang X, Xu H, Abraham SN. A TRP Channel Senses Lysosome Neutralization by Pathogens to Trigger Their Expulsion. Cell. 2015;161: 1306–1319. doi:10.1016/j.cell.2015.05.009

20. O'Hara BA, Morris-Love J, Gee GV, Haley SA, Atwood WJ. JC Virus infected choroid plexus epithelial cells produce extracellular vesicles that infect glial cells independently of the virus attachment receptor. PLOS Pathogens. 2020;16: e1008371. doi:10.1371/journal.ppat.1008371

21. Jiang W, Ma P, Deng L, Liu Z, Wang X, Liu X, et al. Hepatitis A virus structural protein pX interacts with ALIX and promotes the secretion of virions and foreign proteins through exosome-like vesicles. J Extracell Vesicles. 2020;9. doi:10.1080/20013078.2020.1716513

22. Willms E, Cabañas C, Mäger I, Wood MJA, Vader P. Extracellular Vesicle Heterogeneity: Subpopulations, Isolation Techniques, and Diverse Functions in Cancer Progression. Front Immunol. 2018;9. doi:10.3389/fimmu.2018.00738

23. Zhang X, Boyce M, Bhattacharya B, Zhang X, Schein S, Roy P, et al. Bluetongue virus coat protein VP2 contains sialic acid-binding domains, and VP5 resembles enveloped virus fusion proteins. Proc Natl Acad Sci U S A. 2010;107: 6292–6297. doi:10.1073/pnas.0913403107

24. Silvas JA, Paulucci-Holthauzen A, Aguilar PV. Extracellular Vesicles Mediate Receptor-Independent Transmission of Novel Tick-Borne Bunyavirus. Journal of Virology. 2016;90: 873–886. doi:10.1128/JVI.02490-15

25. Raposo G, Stahl PD. Extracellular vesicles: a new communication paradigm? Nat Rev Mol Cell Biol. 2019;20: 509–510. doi:10.1038/s41580-019-0158-7

26. Maclachlan NJ, Drew CP, Darpel KE, Worwa G. The Pathology and Pathogenesis of Bluetongue. Journal of Comparative Pathology. 2009;141: 1–16. doi:10.1016/j.jcpa.2009.04.003

27. Sato M, Tanaka H, Yamada T, Yamamoto N. Persistent infection of BHK21/WI-2 cells with rubella virus and characterization of rubella variants. Archives of Virology. 1977;54: 333–343. doi:10.1007/BF01314778

28. Richter M, Reimann I, Schirrmeier H, Kirkland PD, Beer M. The viral envelope is not sufficient to transfer the unique broad cell tropism of Bungowannah virus to a related pestivirus. Journal of General Virology,. 2014;95: 2216–2222. doi:10.1099/vir.0.065995-0

29. Celma CCP, Roy P. Interaction of Calpactin Light Chain (S100A10/p11) and a Viral NS Protein Is Essential for Intracellular Trafficking of Nonenveloped Bluetongue Virus. J Virol. 2011;85: 4783–4791. doi:10.1128/JVI.02352-10

30. Wirblich C, Bhattacharya B, Roy P. Nonstructural Protein 3 of Bluetongue Virus Assists Virus Release by Recruiting ESCRT-I Protein Tsg101. J Virol. 2006;80: 460–473. doi:10.1128/JVI.80.1.460-473.2006

31. Grein SG van der, Defourny KAY, Rabouw HH, Galiveti CR, Langereis MA, Wauben MHM, et al. Picornavirus infection induces temporal release of multiple extracellular vesicle subsets that differ in molecular composition and infectious potential. PLOS Pathogens. 2019;15: e1007594. doi:10.1371/journal.ppat.1007594

32. Lourenco S, Roy P. In vitro reconstitution of Bluetongue virus infectious cores. Proc Natl Acad Sci U S A. 2011;108: 13746–13751. doi:10.1073/pnas.1108667108

33. Sailleau C, Viarouge C, Bréard E, Perrin JB, Doceul V, Vitour D, et al. Emergence of Bluetongue Virus Serotype 1 in French Corsica Island in September 2013. Transboundary and Emerging Diseases. 2015;62: e89–e91. doi:10.1111/tbed.12207

34. Sailleau C, Bréard E, Viarouge C, Vitour D, Romey A, Garnier A, et al. Re-Emergence of Bluetongue Virus Serotype 8 in France, 2015. Transboundary and Emerging Diseases. 2017;64: 998–1000. doi:10.1111/tbed.12453

35. Mohl B-P, Roy P. Hsp90 Chaperones Bluetongue Virus Proteins and Prevents Proteasomal Degradation. Journal of Virology. 2019;93: e00898-19. doi:10.1128/JVI.00898-19

36. Lv S, Xu Q, Sun E, Yang T, Li J, Feng Y, et al. Autophagy Activated by Bluetongue Virus Infection Plays a Positive Role in Its Replication. Viruses. 2015;7: 4657–4675. doi:10.3390/v7082838

37. Lagache T, Grassart A, Dallongeville S, Faklaris O, Sauvonnet N, Dufour A, et al. Mapping molecular assemblies with fluorescence microscopy and object-based spatial statistics. Nat Commun. 2018;9: 1–15. doi:10.1038/s41467-018-03053-x

Supplemental information

S1 Fig. The majority of BTV virus particles are released in large EVs. (A) Virus particles quantified in the pellet or in the supernatant after isolation of EVs secreted by infected mammalian BSR cells, at 24 or 48 hpi. (B) Intracellular infectivity quantified in infected sheep cells (24 hpi) in presence or absence of an anti syn-7 siRNA. Data are presented as mean ± SD. Each point indicates the value of independent replicates (N = 3; unpaired t-test, ns $p>0.05$, *$p<0.05$, **$p<0.01$).

S1 Table. Total number of lysosomes analysed per time point in sheep cells infected with EVs or free virus particles.

Figure 1

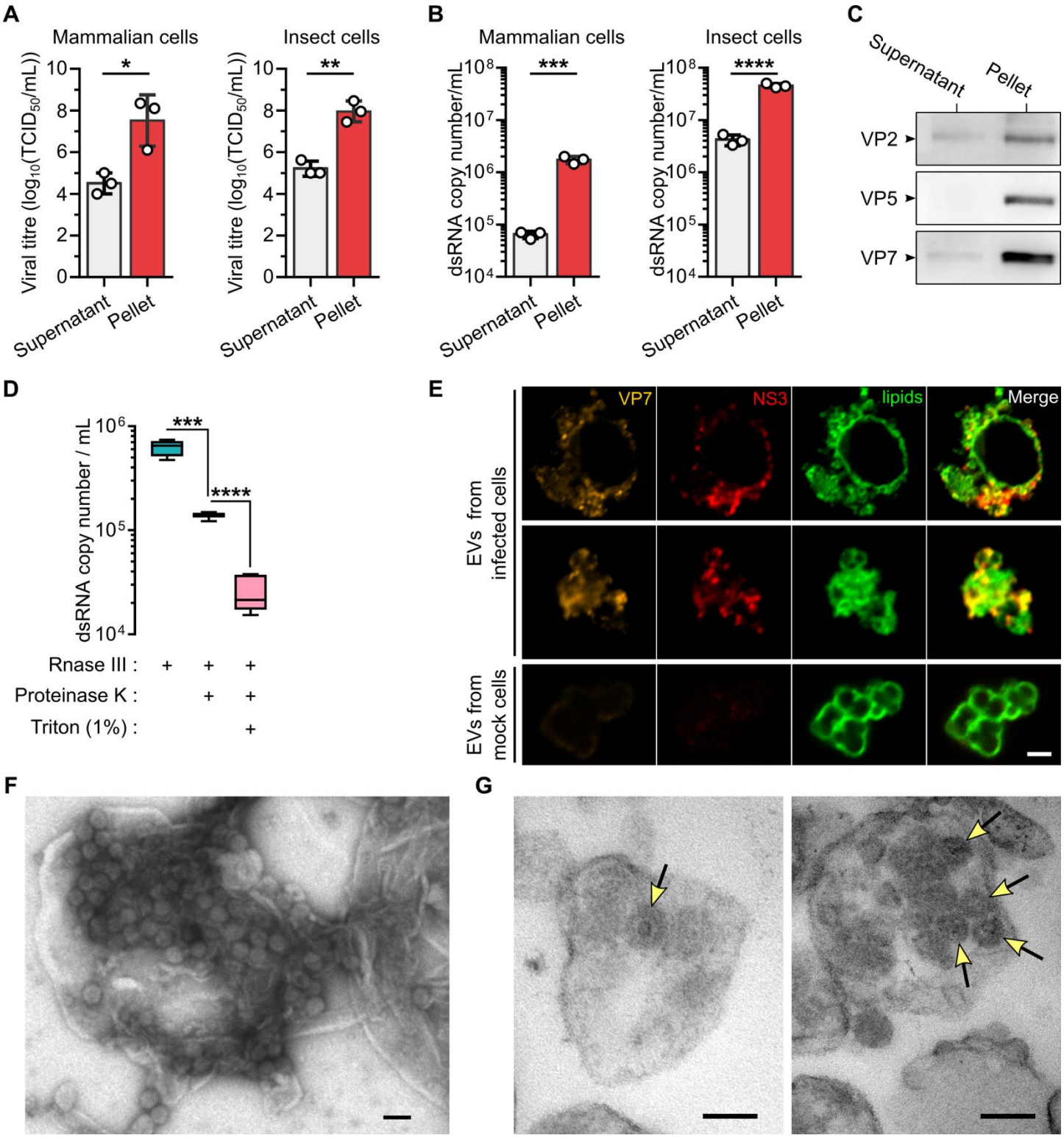
A
Mammalian cells
Insect cells
Viral titre (log10(TCID50/mL))
Supernatant
Pellet
B
dsRNA copy number/mL
C
Supernatant
Pellet
VP2
VP5
VP7
D
dsRNA copy number / mL
Rnase III :
Proteinase K :
Triton (1%) :
E
VP7
NS3
lipids
Merge
EVs from infected cells
EVs from mock cells
F
G

Figure 2

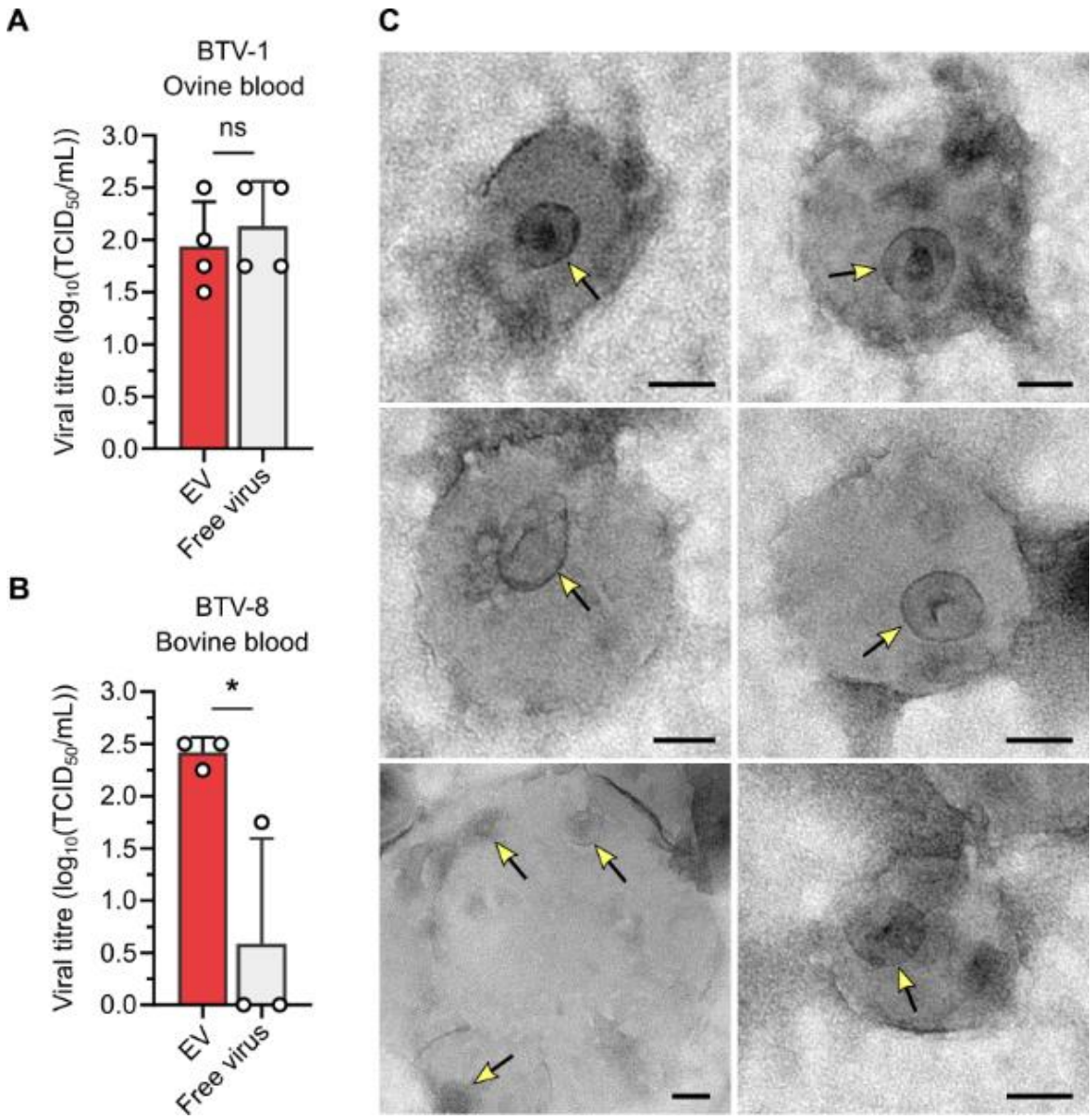
A
BTV-1
Ovine blood
ns
Viral titre (log10(TCID50/mL))
3.0
2.5
2.0
1.5
1.0
0.5
0.0
EV
Free virus
B
BTV-8
Bovine blood
*
Viral titre (log10(TCID50/mL))
3.0
2.5
2.0
1.5
1.0
0.5
0.0
EV
Free virus
C

Figure 3

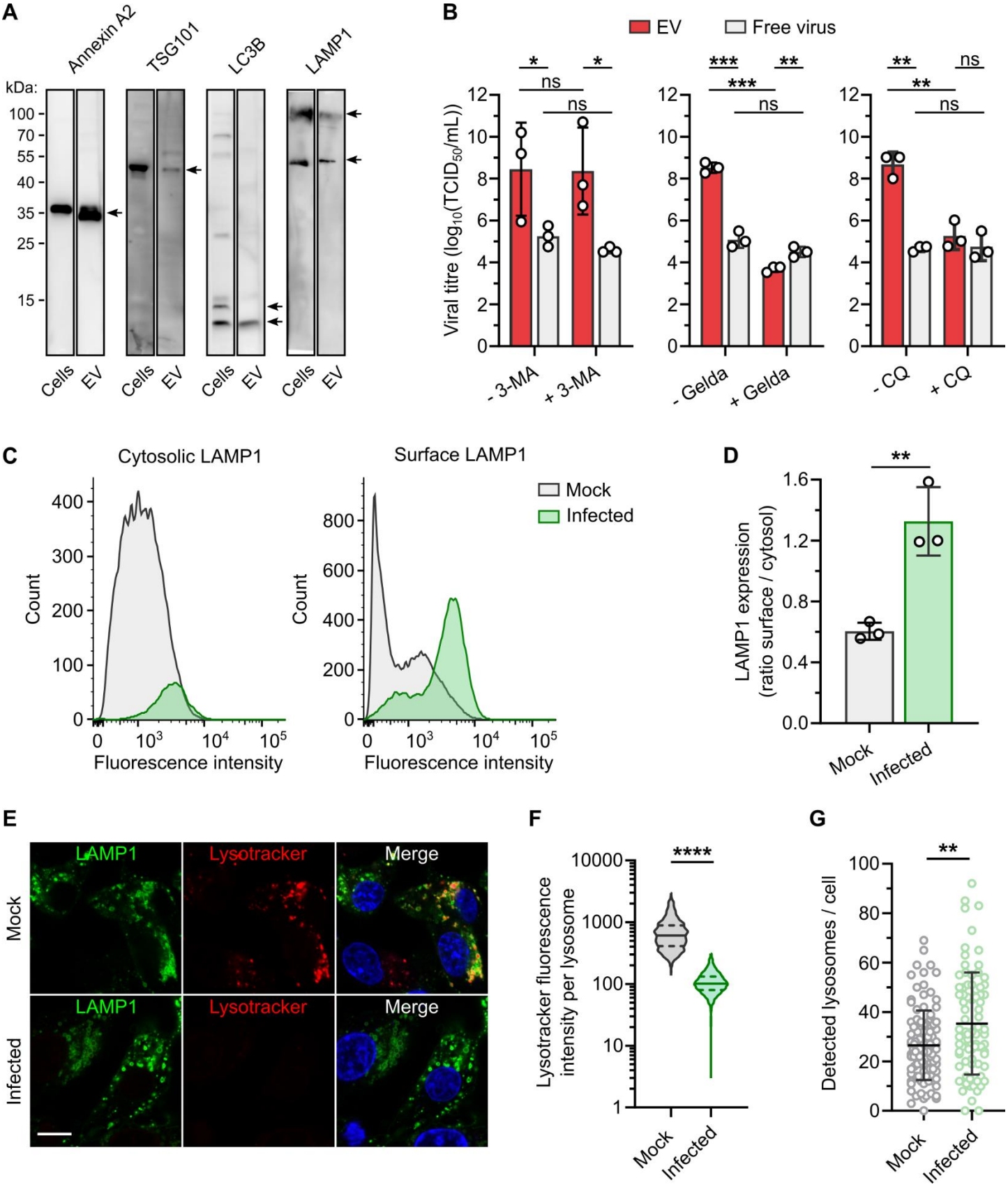
A
Annexin A2
TSG101
LC3B
LAMP1
kDa:
100
70
55
40
35
25
15
Cells
EV
B
EV
Free virus
Viral titre (log10(TCID50/mL))
- 3-MA
+ 3-MA
- Gelda
+ Gelda
- CQ
+ CQ
ns
C
Cytosolic LAMP1
Surface LAMP1
Mock
Infected
Count
Fluorescence intensity
D
LAMP1 expression (ratio surface / cytosol)
Mock
Infected
E
LAMP1
Lysotracker
Merge
Mock
Infected
F
Lysotracker fluorescence intensity per lysosome
G
Detected lysosomes / cell

Figure 4

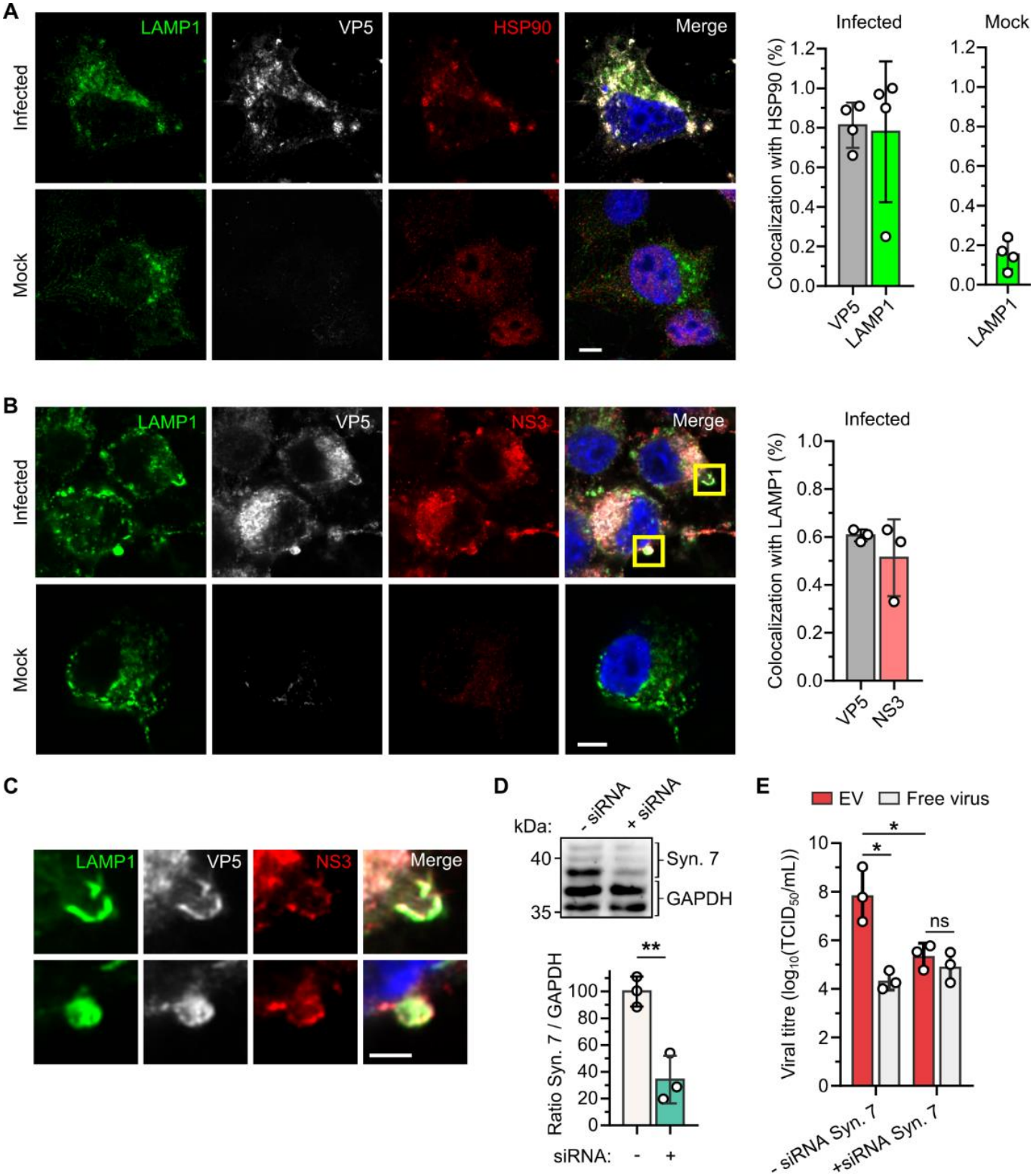
A
LAMP1
VP5
HSP90
Merge
Infected
Mock
Infected
Mock
Colocalization with HSP90 (%)
VP5
LAMP1
LAMP1
B
LAMP1
VP5
NS3
Merge
Infected
Mock
Infected
Colocalization with LAMP1 (%)
VP5
NS3
C
LAMP1
VP5
NS3
Merge
D
kDa:
- siRNA
+ siRNA
40
35
Syn. 7
GAPDH
**
Ratio Syn. 7 / GAPDH
siRNA:
-
+
E
EV
Free virus
*
*
ns
Viral titre (log10(TCID50/mL))
- siRNA Syn. 7
+siRNA Syn. 7

Figure 5

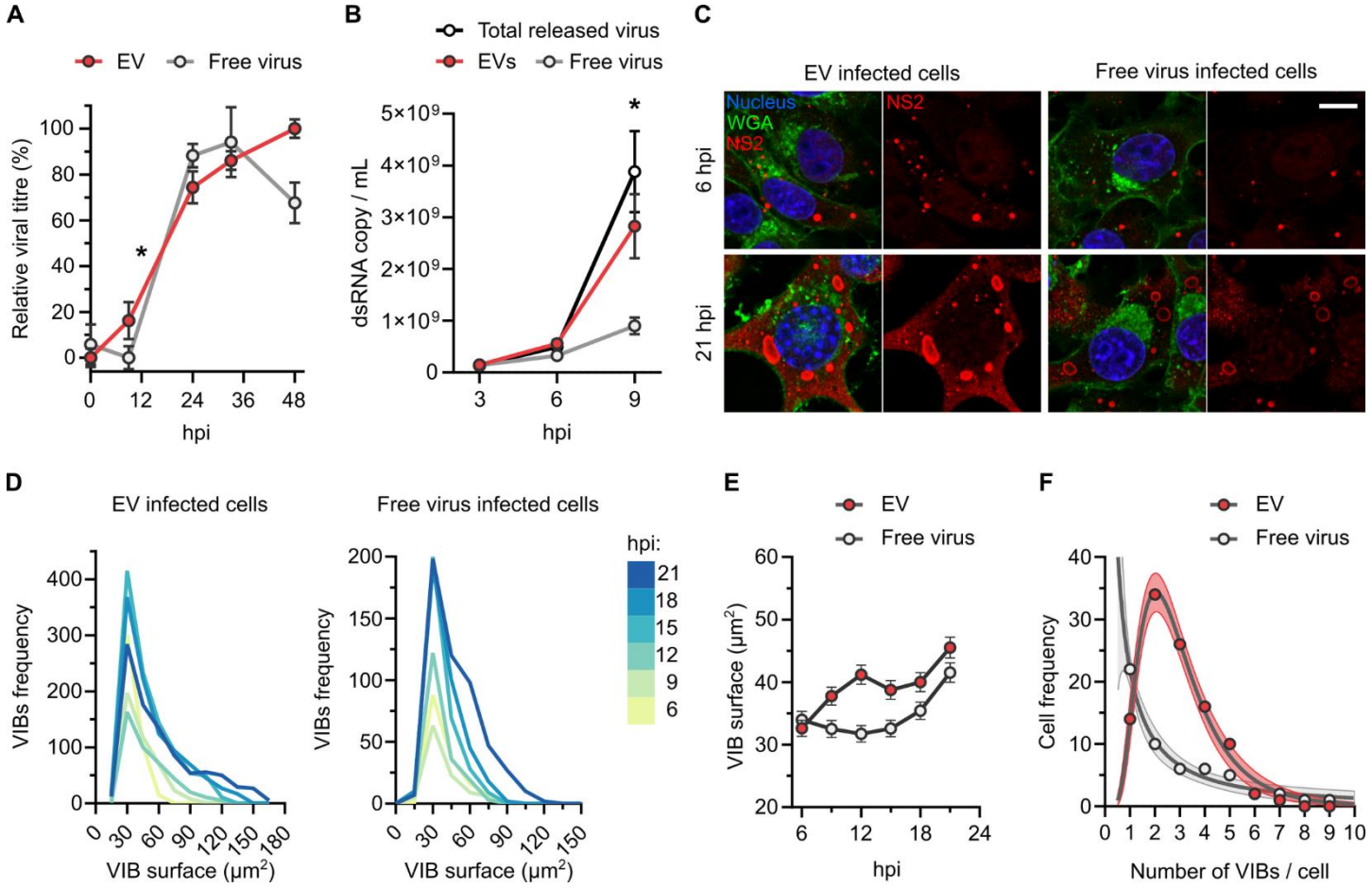
A
EV
Free virus
Relative viral titre (%)
hpi
B
Total released virus
EVs
Free virus
dsRNA copy / mL
hpi
C
EV infected cells
Free virus infected cells
Nucleus
WGA
NS2
6 hpi
21 hpi
D
EV infected cells
Free virus infected cells
VIBs frequency
VIB surface (μm²)
hpi:
21
18
15
12
9
6
E
EV
Free virus
VIB surface (μm²)
hpi
F
EV
Free virus
Cell frequency
Number of VIBs / cell

Figure 6

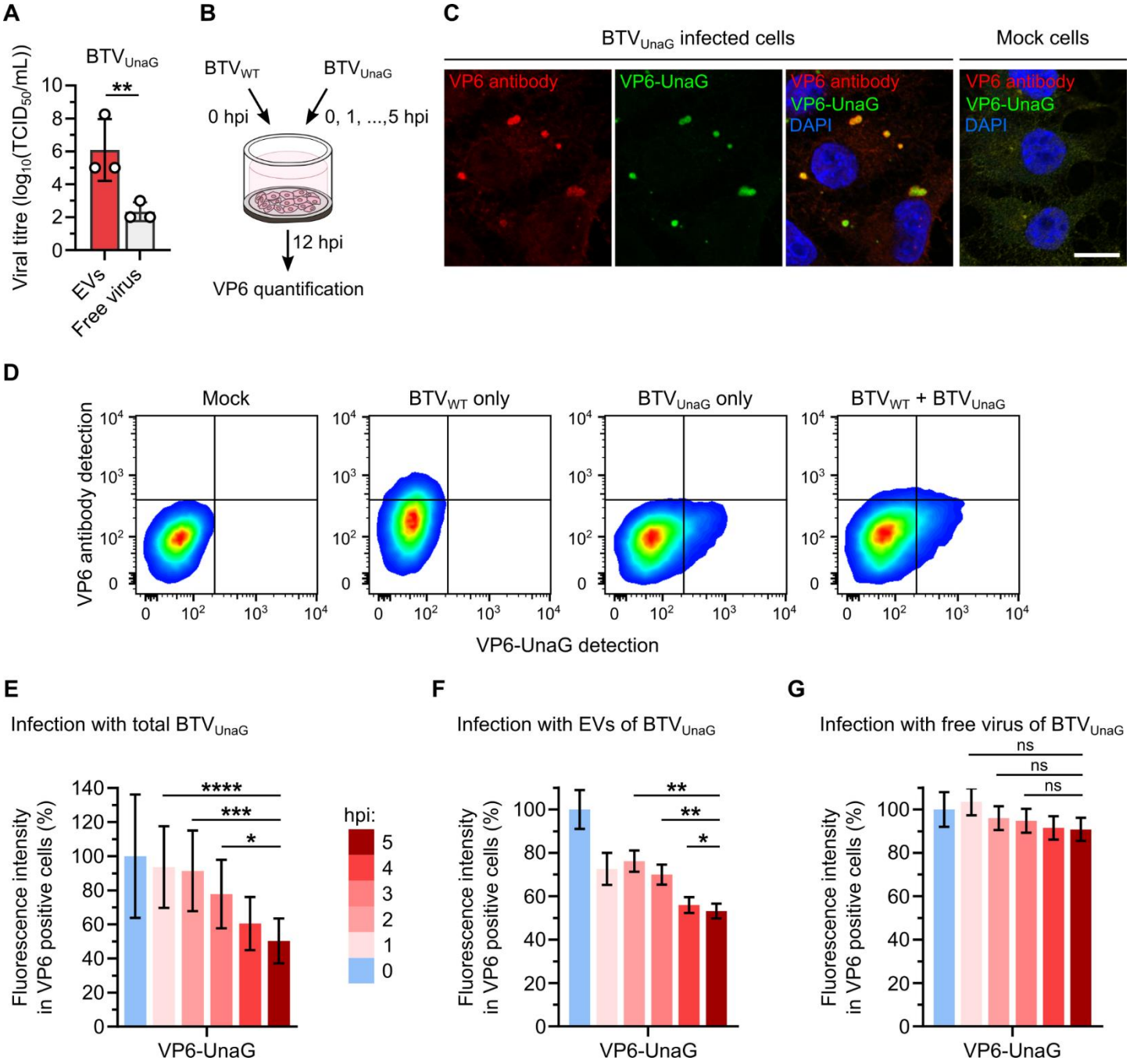
A
BTV$_{UnaG}$
**
Viral titre (log$_{10}$(TCID$_{50}$/mL))
EVs
Free virus
B
BTV$_{WT}$
BTV$_{UnaG}$
0 hpi
0, 1, ...,5 hpi
12 hpi
VP6 quantification
C
BTV$_{UnaG}$ infected cells
Mock cells
VP6 antibody
VP6-UnaG
DAPI
D
Mock
BTV$_{WT}$ only
BTV$_{UnaG}$ only
BTV$_{WT}$ + BTV$_{UnaG}$
VP6 antibody detection
VP6-UnaG detection
E
Infection with total BTV$_{UnaG}$
Fluorescence intensity in VP6 positive cells (%)
****
***
*
hpi:
VP6-UnaG
F
Infection with EVs of BTV$_{UnaG}$
**
**
*
G
Infection with free virus of BTV$_{UnaG}$
ns
ns
ns